Analysis of pairing correlations in neutron transfer reactions and comparison to the constrained molecular dynamics model

C. Agodi,[1,*] G. Giuliani,[2] F. Cappuzzello,[1,2] A. Bonasera,[1,5] D. Carbone,[1] M. Cavallaro,[1] A. Foti,[2,4] R. Linares,[3] and G. Santagati[1]

[1]*INFN - Laboratori Nazionali del Sud, Catania, Italy*

[2]*Dipartimento di Fisica e Astronomia, Università di Catania, Catania, Italy*

[3]*Instituto de Física, Universidade Federal Fluminense, Niteroi, Rio de Janeiro, Brazil*

[4]*INFN, Sezione di Catania, Catania, Italy*

[5]*Cyclotron Institute, Texas A&M University, College Station Texas 77843, USA*

The transfer yields mass spectra were measured in ^{11}B, ^{12,13}C, ^{28}Si(^{18}O,^{17}O) and ^{11}B, ^{12,13}C, ^{28}Si(^{18}O,^{16}O) reactions at 84 MeV. The two-neutron transfer (2NT) and the one-neutron transfer (1NT) cross sections were extracted for all the systems. The 2NT cross section is found comparable to the 1NT one and remarkably larger than that predicted assuming no correlations among the two transferred nucleons and only natural parity states are populated via the (^{18}O,^{16}O) two-neutron transfer reaction. Calculations based on the constrained molecular dynamics model show that such behavior is uniquely a consequence of neutron pairing correlations in the ^{18}O ground state.

I. INTRODUCTION

The observed superconductivity in metals, in which below a critical temperature Cooper pairs of electrons are formed determining a sharp enhancement of the current, is well described by the Bardeen-Cooper-Schrieffer (BCS) theory [1]. Under specific conditions, nuclei can behave in a similar way, despite the reduced number of available nucleons. Hints of superconductivity in nuclei have been widely addressed in the literature [2–7] and attributed to the existence of a nucleonic pairing field on top of the nuclear mean field. Although the scientific interest in such phenomena in finite nuclei and nuclear matter dates back more than a half century, much remains to be investigated [8].

Direct transfer reactions play a polar role in the study of the shell structure in nuclei. In particular, one-nucleon transfer is a selective and direct probe of the single-particle degree of freedom while two-nucleon transfer reactions emphasize pairing correlations in nuclei [9,10]. The effect of the pairing interaction on two-nucleon transfer cross sections has been studied employing semiclassical pictures of heavy ion collision (HICs) [11] and distorted waves Born approximation (DWBA) methods [12,13], many-body approaches such as the Hartree-Fock Bogoliubov (HFB) [14], the time-dependent Hartree-Fock Bogoliubov (TDHFB) [15], and the continuum quasiparticle random phase approximation (cQRPA) [16]. In this paper we apply for the first time the constrained molecular dynamics (CoMD) [17] to nucleon transfer reactions and study the role of pairing correlations. From the experimental side, light-ion induced two-neutron transfer (2NT) reactions have been exploited for decades and the reaction dynamics with light ions is now well understood in terms of the full second order DWBA [18] theory. Heavy-ion induced transfer reactions at energy close to the Coulomb barrier are particularly useful and have attracted large interest for the study of pairing correlations. Indeed their description in terms of semiclassical dynamics allows a direct interpretation of the experimental results [19–25].

This is considerably simplified if the individual final populated states are experimentally resolved. Using thin targets and high-resolution detection systems, such as a magnetic spectrometer, it is possible to well identify the residual nuclei and resolve the final states.

We have already studied the (^{18}O,^{16}O) reaction on several targets, above the Coulomb barrier, and found that this reaction is a powerful tool to give a quantitative indication of the effects of the pairing force in the structure of the atomic nuclei [22,26–31]. The main reason for that is the low polarizability of the ^{16}O core in the ^{18}O ground state, which reduces the active degrees of freedom only to those associated to the two valence neutrons. In addition, significant deviation from the pure $(1d_{5/2})^2$ configuration in the ground state wave function, reported in (p,d), (d,t) one-neutron pick-up reactions [32–35], have been attributed to the presence of pairing correlations. This is also confirmed by shell model calculations [22]. Using the (^{18}O,^{16}O) reaction we have also provided the first experimental indication of the giant pairing vibration [36–38], which is the leading particle-particle giant mode.

Here we show a systematic exploration of the response of ^{11}B, ^{12}C, ^{13}C, and ^{28}Si nuclei to the (^{18}O,^{16}O) probe. We find a remarkable enhancement of 2NT, with respect to 1NT cross sections, attributed to pairing correlations in the ^{18}O ground state wave function.

*Corresponding author: agodi@lns.infn.it

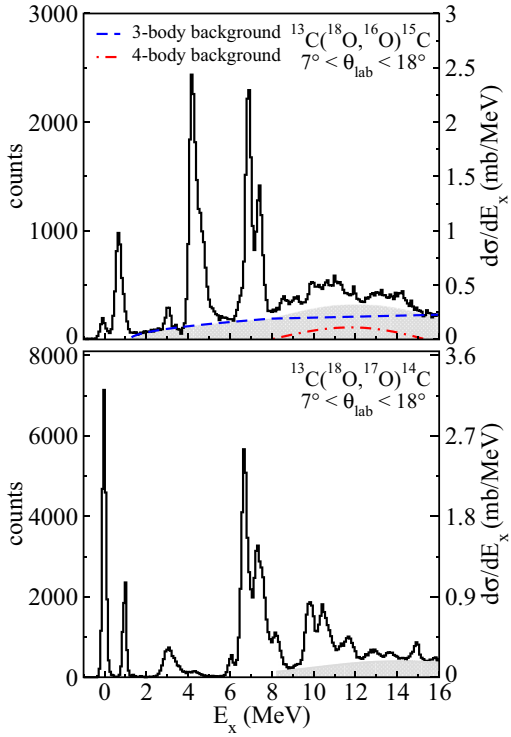


FIG. 1. Examples of the excitation energy spectra for the ^{13}C(^{18}O,^{16}O)^{15}C and ^{13}C(^{18}O,^{17}O)^{14}C reactions at 84 MeV incident energy and $7^\circ < \theta_{lab} < 18^\circ$. The grey area corresponds to the model for the background subtraction (see text). The blue dashed line and the red dashed-dotted lines correspond to the three-body and four-body continuum channels, which open above S_n and S_{2n}, respectively.

II. EXPERIMENTAL TECHNIQUE AND RESULTS

The experiments were performed at INFN-Laboratori Nazionali del Sud (LNS) in Catania. An 84-MeV beam of $^{18}O^{6+}$ ions impinged on thin solid targets. In particular, a $78 \pm 5 - \mu g/cm^2$ self-supporting 97.48% enriched ^{11}B, a $59 \pm 4 - \mu g/cm^2$ self-supporting C, a $50 \pm 3 - \mu g/cm^2$ self-supporting 99% enriched ^{13}C, and a $136 \pm 8 - \mu g/cm^2$ self-supporting Si targets were used. Supplementary runs with a $258 \pm 15 - \mu g/cm^2$ WO_3 on a backing of a $193 \pm 11 - \mu g/cm^2$ Au target were recorded to estimate the background in the spectra coming from oxygen impurities in the ^{11}B and Si targets. The runs with C target were used also to subtract the background coming from impurities of C in the ^{11}B, ^{13}C, and Si targets. The ejectiles, produced in the collisions, were momentum analyzed using the MAGNEX spectrometer [39,40], working in full acceptance mode, $\Omega \sim 50$ msr solid angle and $\Delta p/p = \Delta B\rho/B\rho \sim 24\%$ momentum acceptance, and detected by its focal plane detector [41]. The angular coverage was $7^\circ \leqslant \theta_{lab} \leqslant 18^\circ$ for the $^{18}O + ^{11}B$, $^{18}O + ^{12}C$, and $^{18}O + ^{13}C$ reactions and $3^\circ \leqslant \theta_{lab} \leqslant 14^\circ$ for the $^{18}O + ^{28}Si$ reaction. The data reduction technique, based on a differential algebraic method [42–44], and the performances of the whole system are described in Ref. [40]. A mass resolution of 1/160 was measured [45] and an overall resolution of 160 keV (full width at half maximum) in energy and 0.3° in angle was obtained in the laboratory frame, mainly limited by the multiple scattering in the target and the beam divergence. The cross sections were extracted according to the procedure described in Refs. [37,46]. Examples of the resulting spectra are shown in Fig. 1.

The experimental energy integrated cross section obtained for the one-neutron removal (1NR) and the two-neutron removal (2NR) are listed in Table I. For the ^{12}C and ^{28}Si cases a contribution in the energy spectra is expected also from ^{13}C and ^{29}Si and ^{30}Si present in the natural target, respectively. However, due to the high isotopic abundance of ^{12}C (∼99%) and ^{28}Si (∼92%) such a background is small, especially in the ratio of the integrated cross sections. The indicated error of ±10% is mainly due to the uncertainties in the target thickness and in the integrated beam charge by the Faraday cup. Since the measured spectra are inclusive, in order to obtain the net transfer yield for each reaction channel (2NT and 1NT), the contribution to the yield given by the nonresonant breakup channel should be subtracted. An evaluation of such background for 1NT reactions, in the region above the one-neutron emission threshold S_n, was done using a model function that resembles the uncorrelated three-body continuum, as shown in Fig. 1, lower panel. For 2NT reactions, there is another contribution arising above the two-neutron emission threshold S_{2n}, which was modelled by a least-square approach with different model functions. In Fig. 1, upper panel, an example of such models is shown. The different models do not change the obtained results on the transfer yields within the quoted uncertainties. The results of the transfer yields are listed in Table I as 1NT and 2NT.

Remarkably, the cross sections for 1NT and 2NT are comparable for each investigated target. This trend is not correlated to the Q values of the reactions, also given in Table I. Regardless of any theoretical model, our experimental results show that the 2NT probability is not simply the product of the 1NT independent probabilities.

TABLE I. Total integrated yields and net transfer yields for the different systems. The angular interval is $7^\circ < \theta_{lab} < 18^\circ$ for the $^{18}O + ^{11}B$, $^{18}O + ^{12}C$, and $^{18}O + ^{13}C$ reactions and $3^\circ < \theta_{lab} < 14^\circ$ for $^{18}O + ^{28}Si$. The Q value and the ratios $R = \sigma_{1NT}/\sigma_{2NT}$ and $K = \sigma_{1NR}/\sigma_{2NR}$ for each reaction channel are also listed.

System	^{17}O ejectile				^{16}O ejectile			
	1NR (mb)	1NT (mb)	Q value (MeV)	2NR (mb)	2NT (mb)	Q value (MeV)	$R = \sigma_{1NT}/\sigma_{2NT}$	$K = \sigma_{1NR}/\sigma_{2NR}$
$^{18}O + ^{11}B$	3.2 ±0.3	1.1 ± 0.1	−4.674	2.4 ± 0.2	1.1 ± 0.1	−3.939	0.9 ± 0.2	1.3 ± 0.2
$^{18}O + ^{12}C$	8.3 ±0.8	6.1 ± 0.6	−3.098	7.2 ± 0.7	5.9 ± 0.6	0.935	1.0 ± 0.2	1.1 ± 0.2
$^{18}O + ^{13}C$	11 ±1	8.0 ± 0.8	0.132	7.6 ± 0.7	4.9 ± 0.5	−2.793	1.6 ± 0.3	1.4 ± 0.2
$^{18}O + ^{28}Si$	24 ±2	20 ± 2	0.430	12 ± 1	10 ± 1	6.896	2.0 ± 0.4	2.0 ± 0.3

Furthermore, we observe a clear suppression of unnatural parity states in the even-even systems, indicating a dominant role for no spin-flip dynamics in 2NT. This is particularly evident in the ^{12}C(^{18}O,^{16}O)^{14}C reaction, where the only populated state with unnatural parity (the 2^- at 7.36 MeV) is indeed suppressed [26]. More quantitatively, the integrated cross section for unnatural parity states below S_{2n} accounts for less than 3% of the total, in the same energy interval. The same holds for the reaction ^{28}Si(^{18}O,^{16}O), where the low-lying states are identified as natural parity ones. For high-lying states the experimental resolution is not enough to resolve them. For the odd systems the identification of natural/unnatural parity is less evident. Nevertheless in the case of the ^{15}C it has been shown in Ref. [27] that the most intense populated states correspond to those with a dominant configuration with one neutron orbital coupled to the ^{14}C core natural parity states.

III. THEORETICAL CALCULATIONS

To better investigate the experimental 1NT and 2NT yields we performed calculations based on the constrained molecular dynamics (CoMD) model [17]. The main feature of this model is the constraint on the nucleon one-body phase space occupation probability. The constraint ensures the fermionic nature of nucleons both in the ground state and during the time evolution of nuclear reactions. The CoMD model has been successfully employed in several HIC studies [47–55]. This work shows the first attempt, made within this framework, to determine the neutron transfer absolute cross sections. Such a choice is motivated by some peculiarities of the model, one being the accessibility to all the possible exit channels of a HIC at fixed incident energy and impact parameter. This feature allows the investigation on the competition between 1NT and 2NT processes. Furthermore, the event-by-event dynamics, typical of molecular dynamics models, allows us to use in the calculations the same selection criteria of the experimental data analysis. Nevertheless, compared to more sophisticated theoretical approaches such as DWBA [56–62], coupled channel Born approximation (CCBA) [63–71], and coupled reaction channels [72], molecular dynamics models do not provide information on the detailed level structure of the colliding nuclei. However, since we are interested on energy integrated cross sections, we consider it an acceptable limitation. In the CoMD model each nucleon is described by a Gaussian wave packet in coordinate and momentum space. The effective interaction V employed in CoMD calculations is a function of the superposition integrals between the Gaussian wave packets and it is made up of the following contributions:

$$V = V^{(2)} + V^{(3)} + V^{\mathrm{Sym}} + V^{\mathrm{Coul}} + V^{\mathrm{Surf}}. \qquad (1)$$

$V^{(2)}$ and $V^{(3)}$ represent two- and three-body effective potentials related to the nuclear equation of state parameters $t_0 = -356$ MeV and $t_3 = 303$ MeV which correspond to the isoscalar nuclear compressibility $K_\infty = 200$ MeV [40,42,44]. Such parameters have been first employed in Ref. [73] in the quantum molecular dynamics (QMD) model and further used in CoMD calculations. The symmetry potential V^{Sym} is featured by the strength $S_0 = 32$ MeV and the slope $L = 72$ MeV of the symmetry energy at the saturation density (see Ref. [34]). The Coulomb potential V^{Coul} contains an error function dependence on the coordinates of the protons; the surface potential V^{Surf} is a function of the second derivative in the coordinate space of the superposition integral (for further details on the effective potentials in the CoMD approach see Refs. [40,42–44]).

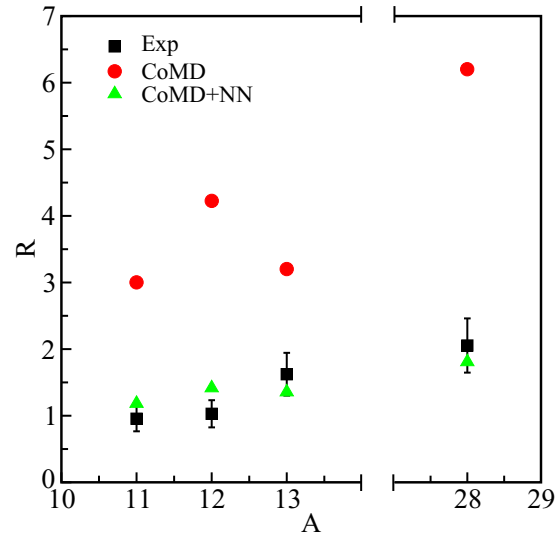


FIG. 2. $R = \sigma_{1\mathrm{NT}}/\sigma_{2\mathrm{NT}}$ for the considered targets. The squares refer to the experimental data, while the circles and the triangles refer to the CoMD and CoMD+NN calculations respectively

The absolute cross sections for 1NT and 2NT processes,

$$\sigma_{1\mathrm{NT(2NT)}} = 2\pi \sum_{b=b_{\min}}^{b_{\max}} P_{1\mathrm{NT(2NT)}}(b) b \Delta b, \qquad (2)$$

have been determined from several thousands of CoMD events generated for the reactions ^{11}B(^{18}O, ^{17,16}O)^{12,13}B, ^{12}C(^{18}O, ^{17,16}O)^{13,14}C, ^{13}C(^{18}O, ^{17,16}O)^{14,15}C, ^{28}Si(^{18}O, ^{17,16}O)^{29,30}Si at 84 MeV laboratory incident energy and for the impact parameter interval $1 \leqslant b \leqslant 9$ fm; the time evolution of the collisions has been followed up to 300 fm/c. The $P_{1\mathrm{NT(2NT)}}(b)$ quantities in Eq. (2) represent the 1NT and 2NT probabilities related to the b impact parameters; $\Delta b = 1$ fm is the impact parameter step.

In Fig. 2, the circles refer to the calculated ratios $R = \sigma_{1\mathrm{NT}}/\sigma_{2\mathrm{NT}}$ between 1NT and 2NT cross sections. The CoMD events have been filtered by the same selection criteria on emission angles and kinetic energies used for the experimental data. The calculated ratios are about 3 for the ^{18}O + ^{11}B and ^{18}O + ^{13}C reactions, in agreement with [74], and greater than 3 for the ^{18}O + ^{12}C and ^{18}O + ^{28}Si reactions. Such values are greater than the experimental ones. We also observe an odd-even staggering behavior between the odd (even)–even (odd) (^{11}B and ^{13}C) and the even-even targets (^{12}C and ^{28}Si).

To understand the origin of the experimental results we have first considered the sensitivity of 1NT and 2NT cross sections and, consequently, of their ratio R on the symmetry potential. The calculations performed for this purpose have shown a weak sensitivity of the R quantity on the values of the slope L ranging from 35 to 145 MeV. A further investigation has been focused

on whether the compound nucleus decay mechanisms might produce one and two neutron-enriched residual nuclei with close probabilities.

Calculations based on the statistical decay model GEMINI [75,76] do not confirm such a hypothesis. The experimental results might represent the evidence of a specific particle-particle correlation which is present in the nuclear ground state, and plays a role in the 2NT processes. More specifically, for the systems under examination, we refer to the neutron-neutron pairing in the ground state of the ^{18}O projectile. To this aim the CoMD model has been implemented by introducing a neutron-neutron pairing interaction. We will refer to this implementation as CoMD+NN.

Particle-particle spatial correlations, related to the Pauli principle and to the folding of the Gaussian wave packets with the terms of Eq. (1) [40], are already present in the CoMD framework. The novel CoMD+NN case adds another particle-particle correlation, which takes place between couples of nucleons having the same isospin (in the present work we consider only neutrons) and opposite spin; such neutron- neutron correlation is the result of the folding of the Gaussian wave packet with a zero range interaction [3–6,14–16] of the form

$$U^{NN} = U_0\delta(r - r')(1 - P_{\sigma,\sigma'}) \quad (3)$$

Equation (3) expresses the pairing interaction operator acting between neutrons near the Fermi momentum P_F. U_0 represents the strength of the interaction, $P_{\sigma,\sigma'}$ is the spin exchange operator. Self-consistent CoMD+NN calculations, which have been performed to reproduce the experimental binding energy and the radius of the ^{18}O nucleus, provide $U_0 = -769.43\,\text{MeV}\,\text{fm}^3$. The neutron pairing gap obtained from these calculations corresponds to $\Delta_n = 3.65\,\text{MeV}$, such value is slightly above the empirical formula $\frac{12}{A^{1/2}} = 2.8\,\text{MeV}$ [4] and greater than the 1.96 MeV value coming from HFB calculations [14]. No fine-tuning of the parameters entering the CoMD model was attempted since it has been rather successful in reproducing diverse experimental data.

The R ratios determined from CoMD+NN events, which have been generated with the same initial conditions of the CoMD ones (incident energy, impact parameters) and also filtered by the experimental selection criteria on emission angles and kinetic energies, correspond to the triangles in Fig. 2. The convergence toward the experimental points is remarkable; we underline that the only difference is represented by the presence of the neutron-neutron pairing interaction. Furthermore, analogously to s-wave pairing, the CoMD+NN pairing interaction occurs only between neutrons having antiparallel spins, therefore the calculations relate only to neutron transfers between natural parity states. Further improvements of the CoMD+NN model will concern the introduction of the pairing interaction and the investigation of transfer processes both in the proton-proton and in the neutron-proton channels.

IV. CONCLUSIONS

Experimental data concerning 1NT and 2NT reactions, collected by the MAGNEX spectrometer at LNS in Catania, have provided values of the ratios $0.9 \leqslant R \leqslant 2$ for all the explored cases. In addition we observe a strong suppression of unnatural parity transitions in the even-even nuclei. The CoMD+NN calculations have shown that measured R values are uniquely a consequence of the neutron-neutron pairing correlations which play a leading role in the 2NT processes. This result could suggest a hint of nuclear superconductivity in (^{18}O,^{16}O) transfer reactions at low energies.

In perspective it is worthwhile to study the same probe (^{18}O,^{16}O) on other heavier and deformed nuclei and to study the same reactions at higher bombarding energies.

ACKNOWLEDGMENTS

The authors gratefully acknowledge all the staff of INFN Laboratori Nazionali del Sud (Catania) for the support during the experiments. This work benefited from services provided to the GRIDIT Virtual Organisation by the national resource providers of the EGI Federation.

[1] L. N. Cooper and D. Feldman, *BCS: 50 Years* (WSPC, Singapore, 2011).
[2] J. H. Bjerrgaard, O. Hansen, O. Nathan, L. Vistisen, R. Chapman, and S. Hinds, Nucl. Phys. A **110**, 1 (1968).
[3] G. F. Bertsch and H. Esbensen, Ann. Phys. **209**, 327 (1991).
[4] D. M. Brink and R. A. Broglia, *Nuclear Superfluidity - Pairing in Finite Systems* (Cambridge University Press, Cambridge, England, Cambridge, 2005).
[5] E. Garrido, P. Sarriguren, E. Moya De Guerra, and P. Schuck, Phys. Rev. C **63**, 037304 (2001).
[6] J. Dobaczewski, W. Nazarewicz, and P. G. Reinhard, Nucl. Phys. A **693**, 361 (2001).
[7] P. J. Borycki, J. Dobaczewski, W. Nazarewicz, and M. V. Stoitsov, Phys. Rev. C **73**, 044319 (2006).
[8] R. A. Broglia and V. Zelevinsky, *Fifty Years of Nuclear BCS. Pairing in Finite Systems* (WSPC, Singapore, 2013).
[9] W. Von Oertzen and A. Vitturi, Rep. Prog. Phys. **64**, 1247 (2001).
[10] C. Y. Wu, W. Von Oertzen, V. Cline, and M. W. Guidry, Annu. Rev. Part. Sci. **40**, 285 (1990).
[11] G. Potel, A. Idini, F. Barranco, E. Vigezzi, and R. A. Broglia, Nucl. Phys. News **24**, 19 (2014).
[12] E. Pllumbi, M. Grasso, D. Beaumel, E. Khan, J. Margueron, and J. Van De Wiele, Phys. Rev. C **83**, 034613 (2011).
[13] J. Lay, L. Fortunato, and A. Vitturi, Phys. Rev. C **89**, 034618 (2014).
[14] M. Grasso, D. Lacroix, and A. Vitturi, Phys. Rev. C **85**, 034317 (2012).
[15] G. Scamps and D. Lacroix, Phys. Rev. C **87**, 014605 (2013).
[16] E. Khan, N. Sandulescu, M. Grasso, and N. Van Giai, Phys. Rev. C **66**, 024309 (2002).

[17] M. Papa, T. Maruyama, and A. Bonasera, Phys. Rev. C **64**, 024612 (2001).
[18] G.R. Satchler, *Direct Nuclear Reactions* (Oxford University Press, New York, 1983).
[19] L. Corradi *et al.*, Phys. Rev. C **54**, 201 (1996).
[20] D. C. Biswas, R. K. Choudhury, D. M. Nadkarni, and V. S. Ramamurthy, Phys. Rev. C **52**, 2827(R) (1995).
[21] D. Pereira *et al.*, Phys. Lett. B **710**, 426 (2012).
[22] M. Cavallaro *et al.*, Phys. Rev. C **88**, 054601 (2013).
[23] F. Cappuzzello, C. Rea, A. Bonaccorso, M. Bondì, D. Carbone, M. Cavallaro, and A. Cunsolo, Phys. Lett. B **711**, 347 (2012).
[24] D. Carbone, M. Bondì, A. Bonaccorso, C. Agodi, F. Cappuzzello, M. Cavallaro, R. J. Charity, A. Cunsolo, M. De Napoli, and A. Foti, Phys. Rev. C **90**, 064621 (2014).
[25] J. R. B. Oliveira *et al.*, J. Phys. G **40**, 105101 (2013).
[26] B. Paes *et al.*, Phys. Rev. C **96**, 044612 (2017).
[27] D. Carbone *et al.*, Phys. Rev. C **95**, 034603 (2017).
[28] M. J. Ermamatov *et al.*, Phys. Rev. C **94**, 024610 (2016).
[29] D. Carbone *et al.*, J. Phys.: Conf. Ser. **312**, 082016 (2011).
[30] D. Nicolosi *et al.*, Acta Phys. Pol. B **44**, 657 (2013).
[31] M. J. Ermamatov *et al.*, Phys. Rev. C **96**, 044603 (2017).
[32] J. C. Legg, Phys. Rev. **129**, 272 (1963).
[33] M. Pignanelli, J. Gosset, F. Resmini, B. Mayer and J. L. Escudié, Phys. Rev. C **8**, 2120 (1973).
[34] G. Mairle, K. T. Knopfle, P. Doll, H. Breuer and G. J. Wagner, Nucl. Phys. A **280**, 97 (1977).
[35] H. T. Fortune, Phys. Rev. C **17**, 861 (1978).
[36] F. Cappuzzello *et al.*, Nat. Commun. **6**, 6743 (2015).
[37] D. Carbone, Eur. Phys. J. Plus **130**, 143 (2015).
[38] M. Cavallaro *et al.*, Phys. Rev. C **93**, 064323 (2016).
[39] A. Cunsolo *et al.*, Eur. Phys. J. ST **150**, 343 (2007).
[40] F. Cappuzzello, C. Agodi, D.Carbone, and M. Cavallaro, Eur. Phys. J. A **52**, 167 (2016).
[41] M. Cavallaro, F. Cappuzzello, D. Carbone, A. Cunsolo, A. Foti, A. Khouaja, M. R. D. Rodrigues, J. S. Winfield, and M. Bondì, Eur. Phys. J. A **48**, 59 (2012).
[42] F. Cappuzzello, D. Carbone, and M. Cavallaro, Nucl. Instrum. Methods Phys. Res. A **638**, 74 (2011).
[43] A. Lazzaro, F. Cappuzzello, A. Cunsolo, M. Cavallaro, A. Foti, S. E. A. Orrigo, M. R. D. Rodrigue, and J. S. Winfield, Nucl. Instrum. Methods Phys. Res. A **591**, 394 (2008).
[44] A. Lazzaro, F. Cappuzzello, A. Cunsolo, M. Cavallaro, A. Foti, A. Khouaja, S. E. A. Orrigo, and J. S. Winfield, Nucl. Instrum. Methods Phys. Res. A **570**, 192 (2007).
[45] F. Cappuzzello *et al.*, Nucl. Instrum. Methods Phys. Res. A **621**, 419 (2010).
[46] M. Cavallaro *et al.*, Nucl. Instrum. Methods Phys. Res. A **648**, 46 (2011).
[47] M. Papa and G. Giuliani, Eur. Phys. J. A **39**, 117 (2009).
[48] H. Zheng, G. Giuliani, and A. Bonasera, Nucl. Phys. A **892**, 43 (2012).
[49] G. Giuliani, H. Zheng, and A. Bonasera, Progr. Part. Nucl. Phys. **76**, 116 (2014).
[50] G. Giuliani and M. Papa, Phys. Rev. C **73**, 031601(R) (2006).
[51] M. Papa and G. Giuliani, Int. J. Mod. Phys. E **20**, 1062 (2011).
[52] M. Papa *et al.*, Phys. Rev. C **72**, 064608 (2005).
[53] F. Amorini *et al.*, Phys. Rev. Lett. **102**, 112701 (2009).
[54] H. Zheng, G. Giuliani, and A. Bonasera, J. Phys. G: Nucl. Part. Phys. **41**, 055109 (2014).
[55] N. Vonta, G. A. Souliotis, M. Veselsky, and A. Bonasera, Phys. Rev. C **92**, 024616 (2015).
[56] R. A. Broglia, C. Ridel, and T. Nagawa, Nucl. Phys. A **135**, 561 (1969).
[57] R. M. Del Vecchio and W. W. Daehnick, Phys. Rev. C **6**, 2095 (1972).
[58] A. J. Baltz and S. Kahana, Phys. Rev. Lett. **29**, 1267 (1972).
[59] B. F. Bayman, Nucl. Phys. A **168**, 1 (1971).
[60] B. F. Bayman, Phys. Rev. Lett. **26**, 157 (1971).
[61] B. F. Bayman, Phys. Rev. Lett. **32**, 71 (1974).
[62] Yu. Ts. Oganessian, V. I. Zagrebaev, and J. S. Vaagen, Phys. Rev. C **60**, 044605 (1999).
[63] T. Tamura, D. R. Bes, R. A. Broglia, and S. Landowne, Phys. Rev. Lett. **26**, 156 (1971).
[64] T. Tamura, Phys. Rep. **14**, 59 (1974).
[65] T. Tamura, K. S. Low, and T. Udagawa, Phys. Lett. B **51**, 116 (1974).
[66] D. Braunschweig, T. Tamura, and T. Udagawa, Phys. Lett. B **35**, 273 (1971).
[67] A. K. Abdallah, T. Udagawa, and T. Tamura, Phys. Rev. C **8**, 1855 (1973).
[68] D. K. Olsen, T. Udagawa, T. Tamura, and R. E. Brown, Phys. Rev. Lett. **30**, 940 (1973).
[69] T. Udagawa, Phys. Rev. C **9**, 270 (1975).
[70] T. Udagawa, T. Tamura, and K. S. Low, Phys. Rev. Lett. **34**, 30 (1975).
[71] M. C. Lemaire and K. S. Low, Phys. Rev. C **16**, 183 (1977).
[72] I. J. Thompson, Comput. Phys. Rep. **7**, 167 (1988).
[73] J. Aichelin, Phys. Rep. **202**, 233 (1991).
[74] L. Corradi *et al.*, Phys. Rev. C **84**, 034603 (2011).
[75] R. J. Charity *et al.*, Nucl. Phys. A **483**, 371 (1988).
[76] R. J. Charity *et al.*, Phys. Rev. C **63**, 024611 (2001).